Available online at www.sciencedirect.com

ScienceDirect

IFAC Papers Online CONFERENCE PAPER ARCHIVE

IFAC-PapersOnLine 49-26 (2016) 289–294

Thermodynamically constrained averaging theory for cancer growth modelling ⋆

Marco Albrecht * **Giuseppe Sciumè** ** **Philippe Lucarelli** * **Thomas Sauter** *

* *University of Luxembourg, Belvaux, 4367 Luxembourg (e-mail: marco.albrecht@uni.lu or thomas.sauter@uni.lu).*
** *University of Bordeaux I2M-TREFLE, Talence Cedex, 33405 France (e-mail: giuseppe.sciume@u-bordeaux.fr)*

Abstract: In Systems Biology, network models are often used to describe intracellular mechanisms at the cellular level. The obtained results are difficult to translate into three dimensional biological systems of higher order. The multiplicity and time dependency of cellular system boundaries, mechanical phenomena and spatial concentration gradients affect the intercellular relations and communication of biochemical networks. These environmental effects can be integrated with our promising cancer modelling environment, that is based on thermodynamically constrained averaging theory (TCAT). Especially, the TCAT parameter viscosity can be used as critical player in tumour evolution. Strong cell-cell contacts and a high degree of differentiation make cancer cells viscous and support compact tumour growth with high tumour cell density and accompanied displacement of the extracellular material. In contrast, dedifferentiation and losing of cell-cell contacts make cancer cells more fluid and lead to an infiltrating tumour growth behaviour without resistance due to the ECM. The fast expanding tumour front of the invasive type consumes oxygen and the limited oxygen availability behind the invasive front results automatically in a much smaller average tumour cell density in the tumour core. The proposed modelling technique is most suitable for tumour growth phenomena in stiff tissues like skin or bone with high content of extracellular matrix.

Keywords: TCAT, Systems Biology, cancer growth, multi phase systems, porous media, tissues

1. INTRODUCTION

The biological field experiences an enormous boost of mathematical and quantitative methods. The field of Systems Biology has emerged in the interface of Molecular Biology, Mathematics, Informatics and Engineering. Besides this movement, a cooperation between mainly clinicians, mathematicians and civil engineers pushed forward the field of Physical Oncology (Frieboes et al. (2011)). During the last five years, those interdisciplinary fields coalesce and mechanics of cancer is more and more related to the biochemical counterparts (Hatzikirou et al. (2012)). Tensile and compressive stress within the tumour arise due to the pressing proliferating tumour mass (Stylianopoulos et al. (2012)) and cells sense these mechanical cues. Some cancer cells react to induced extracellular matrix stiffening with the reinforcement of the own cytoskeleton and increased actin-myosin contractility. This supports the squeezing through the endothelium of blood vessels - a step toward the metastatic aggressive cancer form (Butcher et al. (2009)). The internal cell stiffness follows the stiffness of the environment,*e.g.* via protein tyrosine kinase 2 (PTK2 (FAK)) mediated mechano signal transduction. The mechanical homeostasis is therby regulated by positive and negative feedbacks (Humphrey et al. (2014)). Guck et al. (2005) established a fluidics device that stretches cells with the help of lasers and he points to the softness of several cancer cell lines, especially of metastatic cells. This soft conformation might help cells squeezing through the tight and small channels within the ECM. In melanoma it seems, that the stiffness of the cancer cells changes over the different stages, always using the most appropriate mechanical invasion strategy to circumvent anatomic obstacles (Weder et al. (2014)). This tumour evolutionary pattern has its equivalent phenotype on the transcriptomic pattern. Hoek et al. (2008) state that melanoma cells oscillate between a proliferative but non-invasive and a non-proliferative and invasive phenotype, controlled by Microphthalmia-associated transcription factor (MITF). MITF is a differentiation factor of melanoma. The understanding of the optimal mechanical environment and its modulation might be helpful to improve the therapeutic regimen. Greaves and Maley (2012) emphasize, that chemotherapy removes the poorly adjusted cancer cells first, but resistant cancer clones can remain. These evolutionary selected cells use the cleared space around to grow in an aggressive manner. Some scientists try to limit the available space for tumour growth with cytostatica. Cancer as chronic disease might be better for the patient in some cases, than trying to remove cancer completely. To better analyse these findings, a mathematical model is helpful to understand the mechanical feedback and the concentration gradients in order to minimize the risk and to maximize the therapy success.

In this paper we would like to demonstrate the benefits

⋆ Horizon 2020 MSCA grant agreement No 642295 www.melplex.eu

10.1016/j.ifacol.2016.12.141

of using thermodynamically constrained averaging theory (TCAT) as base for cancer modelling. Following the overview of the modelling framework TCAT, we briefly explain the model characteristics. We demonstrate how tumour cell viscosity can be used as switcher between the invasive and the non-invasive tumour type and finally we will show why our modelling approach is ideally suited to be coupled with the network models in Systems Biology. Thereby, we focus on the description of biological compartments and the cellular sensors, which react to the mechanical state of a tissue. Moreover, we discuss cellular functions modifying the mechanical state of the tissue.

2. THERMODYNAMICALLY CONSTRAINED AVERAGING THEORY

Several phenomena in geology, hydrology, petroleum engineering and technology deal with porous media in which multiphase flows occur. Gases and immiscible liquids flow faster than the solid bulk material or stone. Usually Darcy's law is applied. But this is a formulation on the macroscale only. Several microscale phenomena like wettability have a significant impact on the macroscale but are not mathematically considered (Sciumè et al. (2013)). These inconsistencies are frequently bridged with pure mathematical constructs without physical relations. The thermodynamically constrained averaging theory (TCAT), as developed by Gray and Miller (2014), is a rigorous methodology to interconnect conservation equations across different length scales. Conservation equations of phases, interphases, common curves and common points are represented in material derivative form and integrated in the entropy inequality equation. The entropy inequality is then maximized in a Langrangian framework, constrained by the conservation equations to obtain a constrained entropy inequality. Variational methods are used to find closure relations near equilibrium. Force-flux pairs in the constrained entropy inequality can be used to reduce the system, because each pair must equal zero. Averaging theorems are used to transfer microscale equations to macroscale equivalents and evolution equations account for the maintenance of geometric properties.

3. TCAT TISSUE MODEL DEFORMED BY TUMOUR GROWTH

The use of TCAT eases the formulation of a model describing tumour growth. The framework allows a straight forward model extension using partial differential equations with at most second order derivatives in time and space. Other methods in the field of continuous modelling like mixture theory are confronted with complicated fourth order Cahn Hilliard equations and are difficult to extent (Sciumè et al. (2013)). TCAT was applied by Giuseppe Sciumè *et. al.* to investigate the impact of mechanical stress on diabetic foot ulceration (Sciumè et al. (2014a)) and to explain tumour growth within healthy tissues. This section summarizes the latest model of melanoma growth in skin from Sciumè et al. (2014b) with some minor modifications as detailed below.

The solid porous medium represents the ECM, a protein network secreted by the cells to establish a stable cell environment. This ECM contains tortuous interconnected gaps, whose volume taken together is called porosity ϵ. The saturation degree S^α states how these pores are saturated with three immiscible liquids α, representing interstitial fluid (IF,l), host cell population (HC,h) and tumour cell population (TC,t). Favourable growth conditions for the tumour cells lead to TC mass expansion by converting IF to TC. The expanding TC liquid presses against the other fluids and the ECM. The ECM has a general permeability $\mathbf{k}$ for liquids, depending on the tissue characteristic. A relative permeability k^α_{rel} represents the migration of a cell phase in relation to the others, while the IF moves last because it's more attached to the ECM (high wettability or hydrophilicity). From the TCAT momentum equation we obtain a relationship between the fluid velocity $\mathbf{v}^{\overline{\alpha}}$ relative to the ECM scaffold velocity $\mathbf{v}^{\overline{s}}$

$$\mathbf{v}^{\overline{\alpha}} - \mathbf{v}^{\overline{s}} = \frac{k^\alpha_{rel}\mathbf{k}}{\mu^\alpha S^\alpha \epsilon} \cdot (-\nabla p^\alpha) \qquad (\alpha = h, t, l). \tag{1}$$

The velocity difference depends on the pressure gradient $(-\nabla p^\alpha)$. The dynamic viscosity μ^α of the cell population represents their ability to be moved. This movement is inhibited by cell-cell contacts modelled with high viscosity up to a pressure gradient threshold. After exceeding this pressure gradient threshold, the cell-cell contacts unbound and the viscosity is assumed to be reduced smoothly by a factor of ten.

The tissue model can be formulated at the macro-scale and is derived from TCAT mass conservation and momentum conservation equations. The five primary variables are the oxygen concentration $\omega^{\overline{ol}}$, the pressure of the IF phase p^l, the pressure difference between IF and HC phase p^{hl}, and the pressure between TC and HC phase p^{th} - while the sum of these pressures corresponds to the tumour pressure $p^t = p^l + p^{hl} + p^{th}$. The displacement of the extracellular matrix $\mathbf{u}^s$ is the fifth primary variable.

The momentum balance equation of the extracellular matrix is

$$\nabla \cdot \left(\frac{\partial \mathbf{t}^{\overline{\overline{s}}}_{\text{eff}}}{\partial t} - \frac{\partial p^s}{\partial t} \right) = 0. \tag{2}$$

The effective stress rate is defined as $\dot{\mathbf{t}}^{\overline{\overline{s}}}_{\text{eff}} = \mathbf{D}_s : \dot{\mathbf{e}}^{\overline{\overline{s}}}_{\text{el}} = \mathbf{D}_s : (\dot{\mathbf{e}}^{\overline{\overline{s}}} - \dot{\mathbf{e}}^{\overline{\overline{s}}}_{\text{vp}})$, where the strain rate $\dot{\mathbf{e}}^{\overline{\overline{s}}} = \mathbf{S}\frac{\partial \mathbf{u}^s}{\partial t}$ is of visco-plastic (vp) and elastic (el) origin. The tangent matrix $\mathbf{D}_s$ represents the mechanical properties of the ECM and links the stress with the strain, while tensor $\mathbf{S}$ links the strain with the displacement. The solid pressure is coupled with the proportionately considered liquid pressures $p^s = p^l + (1 - S^l)p^{hl} + S^t p^{th}$, using pore saturation S^α as Bishop parameter. The result is the pressure-strain relationship $\frac{\bar{\alpha}}{K}\frac{\partial p^s}{\partial t} = \mathbf{1} : \mathbf{d}^{\overline{\overline{s}}}_{sp}$. Each liquid and solid component is not compressible but the deformation of the ECM scaffold is taken into account by bulk modulus K. The final governing ECM displacement equation, based on Equation 2, is

$$\nabla \cdot (\mathbf{D}_s : (\mathbf{S}\frac{\partial \mathbf{u}^s}{\partial t})) - \nabla \cdot (\mathbf{D}_s : \dot{\mathbf{e}}^{\overline{\overline{s}}}_{vp}) = \nabla \cdot (\mathrm{K}(1 : \dot{\mathbf{e}}^{\overline{\overline{s}}}_{sp})). \tag{3}$$

The mass balance equation of the solid phase is integrated in the following mass balance equations of three immiscible liquids: The interstitial fluid phase

$$\begin{aligned}
&\left[\frac{1}{K}(S^t + p^{th}\frac{\partial S^t}{\partial p^{th}})\right]\frac{\partial p^{th}}{\partial t} \\
&+ \left[\frac{1}{K}(1 - S^l - p^{hl}\frac{\partial S^l}{\partial p^{hl}})\right]\frac{\partial p^{hl}}{\partial t} + \left[\frac{1}{K}\right]\frac{\partial p^l}{\partial t} \\
&= \nabla\cdot\left[\frac{k^t_{rel}\mathbf{k}}{\mu^t}\cdot\nabla p^{th}\right] + \nabla\cdot\left[\left(\frac{k^t_{rel}\mathbf{k}}{\mu^t} + \frac{k^h_{rel}\mathbf{k}}{\mu^h}\right)\cdot\nabla p^{hl}\right] \\
&+ \nabla\cdot\left[\left(\frac{k^t_{rel}\mathbf{k}}{\mu^t} + \frac{k^h_{rel}\mathbf{k}}{\mu^h} + \frac{k^l_{rel}\mathbf{k}}{\mu^l}\right)\cdot\nabla p^{l}\right] \\
&- \left[\mathbf{1}:(\dot{\boldsymbol{\varepsilon}}^{\overline{\overline{s}}} - \dot{\boldsymbol{\varepsilon}}^{\overline{\overline{s}}}_{sp})\right] + \frac{\rho^l - \rho^t}{\rho^t\rho^l}\overset{l\to t}{\mathrm{M}},
\end{aligned} \tag{4}$$

the host cell phase

$$\begin{aligned}
&\left[\frac{S^h}{K}(S^t + p^{th}\frac{\partial S^t}{\partial p^{th}}) - \epsilon\frac{\partial S^t}{\partial p^{th}}\right]\frac{\partial p^{th}}{\partial t} \\
&+ \left[\frac{S^h}{K}(1 - S^l - p^{hl}\frac{S^l}{p^{hl}}) - \epsilon\frac{\partial S^l}{\partial p^{hl}}\right]\frac{\partial p^{hl}}{\partial t} + \left[\frac{S^h}{K}\right]\frac{\partial p^l}{\partial t} \\
=&\nabla\cdot\left[\frac{k^h_{rel}\mathbf{k}}{\mu^h}\cdot\nabla(p^l + p^{hl})\right] - S^h\left[\mathbf{1}:(\dot{\boldsymbol{\varepsilon}}^{\overline{\overline{s}}} - \dot{\boldsymbol{\varepsilon}}^{\overline{\overline{s}}}_{sp})\right] - \epsilon\mathbf{v}^{\overline{s}}\nabla S^h,
\end{aligned} \tag{5}$$

and the tumour cell phase

$$\begin{aligned}
&\left[\frac{S^t}{K}(S^t + p^{th}\frac{\partial S^t}{\partial p^{th}}) + \epsilon\frac{\partial S^t}{\partial p^{th}}\right]\frac{\partial p^{th}}{\partial t} \\
&+ \left[\frac{S^t}{K}(1 - S^l - p^{hl}\frac{\partial S^l}{\partial p^{hl}})\right]\frac{\partial p^{hl}}{\partial t} + \left[\frac{S^t}{K}\right]\frac{\partial p^l}{\partial t} \\
=&\nabla\cdot\left[\frac{k^t_{rel}\mathbf{k}}{\mu^t}\cdot\nabla(p^l + p^{hl} + p^{th})\right] - S^t\left[\mathbf{1}:(\dot{\boldsymbol{\varepsilon}}^{\overline{\overline{s}}} - \dot{\boldsymbol{\varepsilon}}^{\overline{\overline{s}}}_{sp})\right] \\
&- \epsilon\mathbf{v}^{\overline{s}}\nabla S^t + \frac{1}{\rho^t}\overset{l\to t}{\mathrm{M}}.
\end{aligned} \tag{6}$$

The tumour cell phase can be partitioned in two miscible liquids accounting for the living tumour cell fraction $(1 - \omega^{\overline{Nt}})$ and the necrotic tumour cell fraction

$$\frac{\partial\omega^{N\bar{t}}}{\partial t} = \frac{1}{\epsilon S^t\rho^t}\left[\epsilon S^t r^{Nt} - \omega^{N\bar{t}}\underset{\text{growth}}{\overset{l\to t}{\mathrm{M}}} - \epsilon S^t\rho^t\mathbf{v}^t\cdot\nabla\omega^{N\bar{t}}\right], \tag{7}$$

which arises with a low oxygen mass fraction ω^{ol}, whose distribution is described by species mass conservation equation

$$\epsilon S^l\frac{\partial\omega^{ol}}{\partial t} = \nabla\cdot(\epsilon S^l D_0^{\overline{ol}}(\epsilon S^l)^\sigma\nabla\omega^{ol}) + \frac{1}{\rho^l}(\omega^{ol}\overset{l\to t}{\mathrm{M}} - \overset{ol\to t}{\mathrm{M}}) \tag{8}$$

with the oxygen diffusion coefficient $D_0^{\overline{ol}}$. The mass transfer from the IF phase to the TC phase $\mathrm{M}^{l\to t}$ is related to tumour growth using free IF from the environment. The related oxygen species transfer $\mathrm{M}^{ol\to t}$ account for the oxygen consumption. Cell death due to oxygen limitation is modelled as species transfer r^{Nt} between two miscible liquids. The living tumour mass is transferred to the fraction of dead tumour mass within the immiscible tumour cell phase. These three transfer terms are composed of cosine functions 9 to 12 containing threshold parameters that describe the transition zones between minimum and maximum tumour growth, oxygen consumption, and tumour cell death rates.

$$G_1(\omega^{\overline{ol}}) = \begin{cases} 0 & \text{for } 0 \le \omega^{\overline{ol}} \le \omega^{\overline{ol}}_{\text{crit}} \\ \frac{1}{2} + \frac{1}{2}\cos\left[\pi\left(1 + \frac{\omega^{\overline{ol}} - \omega^{\overline{ol}}_{\text{crit}}}{\omega^{\overline{ol}}_{\text{env}} - \omega^{\overline{ol}}_{\text{crit}}}\right)\right] & \text{for } \omega^{\overline{ol}}_{\text{crit}} \le \omega^{\overline{ol}} \le \omega^{\overline{ol}}_{\text{env}} \\ 1 & \text{for } \omega^{\overline{ol}} \ge \omega^{\overline{ol}}_{\text{env}} \end{cases} \tag{9}$$

$$G_2(p^t) = \begin{cases} 1 & \text{for } 0 \le p^t \le p^t_{\text{cr1}} \\ \frac{1}{2} + \frac{1}{2}\cos\left[\pi\left(1 + \frac{p^t - p^t_{\text{cr1}}}{p^t_{\text{cr2}} - p^t_{\text{cr1}}}\right)\right] & \text{for } p^t_{\text{cr1}} \le p^t \le p^t_{\text{cr2}} \\ 0 & \text{for } p^t \ge p^t_{\text{cr2}} \end{cases} \tag{10}$$

$$R(\omega^{\overline{ol}}) = \begin{cases} \frac{1}{2} + \frac{1}{2}\cos\left[\pi\left(1 + \frac{\omega^{\overline{ol}}}{\omega^{\overline{ol}}_{\text{crit}}}\right)\right] & \text{for } 0 \le \omega^{\overline{ol}} \le \omega^{\overline{ol}}_{\text{crit}} \\ 1 & \text{for } \omega^{\overline{ol}} \ge \omega^{\overline{ol}}_{\text{crit}} \end{cases} \tag{11}$$

$$N_1(\omega^{\overline{ol}}) = \begin{cases} \frac{1}{2} + \frac{1}{2}\cos\left(\frac{\omega^{\overline{ol}}}{\omega^{\overline{ol}}_{\text{crit}}}\pi\right) & \text{for } 0 \le \omega^{\overline{ol}} \le \omega^{\overline{ol}}_{\text{crit}} \\ 0 & \text{for } \omega^{\overline{ol}} \ge \omega^{\overline{ol}}_{\text{crit}} \end{cases} \tag{12}$$

Below the oxygen threshold $\omega^{\overline{ol}}_{\text{crit}}$, the tumour cells have a reduced basic respiratory or metabolic turnover rate with basic oxygen consumption rate $R(\omega^{\overline{ol}})$ and start to die, while above this threshold, tumour cells start growing until they reach the maximum proliferation rate at the environmental oxygen concentration $\omega^{\overline{ol}}_{\text{env}}$. The proliferation rate is maximal if tumour pressure is below p^t_{cr1}. Above this threshold, cells have a reduced growth rate to mimic contact inhibition.

Necrosis is a process, that shuts down the work of ion pumps due to energy shortage. Osmotic water influx lets the necrotic tumour cells swell within 3 hours to the doubled size, before the cells lose water through a stretched and leaky cell membrane. The concentrated cytoplasm builds calcified crystals, accumulating in the necrotic core of tumours (Macklin et al. (2013)). Accordingly, the swelling can be modelled with a factor of two in the necrosis rate equation

$$\epsilon S^t r^{N^t} = 2\cdot[\gamma^t_{\text{necrosis}}N_1(\omega^{\overline{ol}})](1 - \omega^{N\bar{t}})\epsilon S^t - \gamma^t_{\text{clear}}\omega^{N\bar{t}}\epsilon S^t. \tag{13}$$

Equation 13 contains the maximal necrosis rate $\gamma^t_{\text{necrosis}}$ and an additional term describing cell degradation with clearance rate γ^t_{clear}. Because this is only a transfer within the tumour phase, the tumour growth rate has to be adjusted, so that the necrotic swelling arises from the interstitial fluid and not from the living tumour mass $(1 - \omega^{N\bar{t}})\epsilon S^t$. The growth rate

$$\begin{aligned}
\overset{l\to t}{\underset{\text{growth}}{\mathrm{M}}} =&[\gamma^t_{\text{growth}}G_1(\omega^{\overline{ol}})G_2(p^t)](1 - \omega^{\overline{Nt}})\epsilon S^t \\
&+ [\gamma^t_{\text{necrosis}}N_1(\omega^{\overline{ol}})](1 - \omega^{N\bar{t}})\epsilon S^t \\
&- \gamma^t_{\text{clear}}\omega^{N\bar{t}}\epsilon S^t
\end{aligned} \tag{14}$$

with maximal growth rate γ^t_{growth} can be increased by the swelling of the necrotic fraction and can be reduced due to the shrinkage and degradation of the necrotic material. The swelling and degradation of necrotic material are extensions for the model from Sciumè et al. (2014b) while Equations 9 - 12 replace former used Heaviside step functions for a better numeric stability.

The model equations are discretized in space with Galerkin and in time with the approach of Crank-Nicolson using the

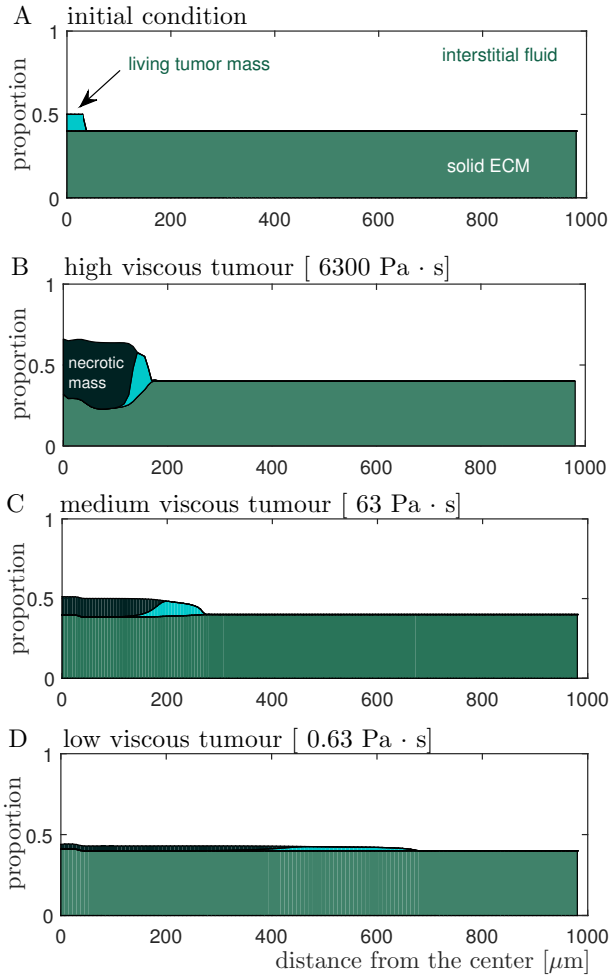

Fig. 1. Volume proportions of solid ECM (dark green), interstitial fluid (white), living tumour mass (cyan) and the necrotic core (black) changes along the spheroid radius. The left side is the micro tumour spheroid core. **A:** Initial condition. **B-D:** Model simulation of tumour growth with high (B), medium (C) and low (D) viscosity after 31 days. The change of the viscosity is comparable with a switch between benign and malignant tumour growth.

Wilsons Theta method. The equations are implemented in Cast3M (www-cast3m.cea.fr) and solved with a finite element method. The mathematical model contains two blocks: One describes pressure and diffusion with Equations 4, 5, 6 and 8; and one takes into account the solid mechanics with Equation 3. Both blocks are solved iteratively, until convergence is reached at each single time step.

4. SIMULATION RESULTS

A physical model of cancer growth should explain biological phenomena observed experimentally. One important experimental observation is the change from a compact growing tumour to an invasive tumour with reduced growth. In this paper, the tumour evolution is investigated when cell-cell contacts are weakened and intracellular stiffness is decreased. Accordingly, three different viscosities are simulated for the tumour cell phase: The high viscous tumour ($\mu^t = 6300$ Pa · s), the medium viscous tumour ($\mu^t = 63$ Pa · s) and the low viscous tumour ($\mu^t = 0.63$ Pa · s).

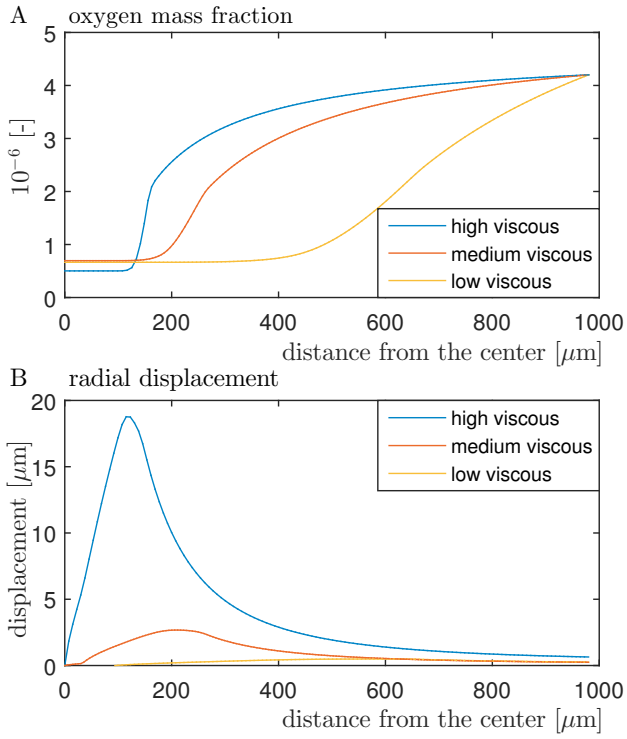

Fig. 2. Spatial profile along the radius after 31 days simulated. **A:** Oxygen mass fraction (unitless). **B:** ECM displacement. Positive displacement means a displacement in direction of the spheroid surface while a negative sign indicates a compression in direction tumour center.

The starting condition is illustrated in Figure 1 A. An initial tumour mass (radius: 50 μm) in a three dimensional collagen gel spheroid (radius: 1000 μm) has been defined. After the simulation of 31 days, three different viscosities yield three clearly different tumour phenotypes. Exact values are listed in Table 1.

The high viscous tumour grows compact and slow (Figure 1 B) and 33.5 % of the cells are alive.

The medium viscous tumour infiltrates a 46% larger radius and a 3 times bigger volume. The absolute tumour cell

Table 1. Final results after 31 days of simulation. The space infiltrated by the tumour contains, besides the tumour cells, interstitial fluid and ECM. The cytoplasm volume of all dead and living tumour cells (TC) or of all living tumour cells (LTC) is lower. The displacement of the ECM decreases with lower viscosity.

	high viscous tumour	medium viscous tumour	low viscous tumour
Radius infiltrated [μm]	199	291	695
Volume infiltrated [mm^3]	33	103	1408
Volume of TC [$10^{-3} mm^3$]	8.55	8.73	33.32
Volume of LTC [$10^{-3} mm^3$]	2.86	5.31	23.67
Max displacement [μm]	18.8	2.68	0.49

volume remains almost constant, while the fraction of living cells is with 60.8% distinctly larger. The tumour cell density is clearly smaller (Figure 1 C).
The low viscous tumour infiltrates a 3.5 times larger radius than the high viscous tumour and it infiltrates a 42.7 larger volume. The absolute tumour mass increases by a factor of 3.9. Figure 1 D indicates the very small tumour cell density. The low viscous tumour has the largest necrotic core with a radius of around 400 μm and has the thickest living tumour front with 295 μm. 71% of the low viscous tumour mass belongs to the living tumour cell mass.
The correlation between viscosity and tumour cell density can be explained with the oxygen mass fraction. The oxygen profiles of all three cases are shown in Figure 2 A and the profile of each case can be separated in three sections. The first section is located in the necrotic core zone in which the oxygen mass fraction is constant at minimum level. The second section is in the zone of the living tumour cell front. Here, the biggest change of the oxygen mass fraction is observed. The third section is the zone of the pure gel. The profile of the oxygen mass fraction in the third zone depends on diffusion. The oxygen mass fraction increases from the invasive front to the fixed value of $4.2 \cdot 10^{-6}$ at the boundary of the collagen spheroid. The more viscous the tumour is, the more time the tumour has to grow locally. In the low viscous case, the living tumour front changes the position quickly. At the new position, the living tumour front consumes oxygen and interrupts the supply of oxygen for the old position behind. The tumour become faster necrotic than in the viscous case and the cell density remains small.
Figure 2 B shows the displacement of the ECM due to the growing tumour. The high viscous tumour displaces the surrounding ECM by almost 20 μm. This could explain the lower oxygen level in the necrotic core in comparison to the less viscous cases. The compressed matrix reduces the pore space for diffusion and the sharp living tumour front takes more from the remaining oxygen of the tumour zone instead of the tumour environment. The displacement decreases from the high viscous to the medium viscous tumour by a factor of 7 and from the medium viscous to the low viscous tumour by a factor of 5.5, according Table 1. Within medium and low viscous tumours, cells can squeeze easier through the ECM and the solid ECM has a lower resistance to tumour growth. While in the solid tumour, ECM has an impact, the displacement of the ECM for the medium and low viscous growth is negligible and no limitation of oxygen delivery is expected due to compressed ECM.

5. DISCUSSION

The change of the viscosity is like the change between benign and malign tumour growth. The question is, whether it is easier for the tumour to displace or to flow through the ECM in order to grow. The observed smoothness in cancer cell lines by Guck et al. (2005) has also in our simulation a profound benefit for the tumour evolution. The low viscous tumour has infiltrated a much larger space than the high viscous tumour, representing stiff and highly differentiated cancer cells with strong cell-cell contacts. But the dedifferentiation of melanoma cells - that supports this invasive growth - is also connected at the molecular level with a reduced growth rate (Hoek et al. (2008)), which will be considered for the model in subsequent papers. Our model predicts a much lower cancer cell density in accordance with the related oxygen profile for the invasive tumour, although the molecular link between dedifferentiation and growth rate has been neglected. Hoek et al. (2008) discovered in the flanks of mice, that the invasive tumour grows slower than the proliferative phenotype. But their result might be underestimated as dedifferentiated cancer cells cannot be stained specifically and because the tumour size measurement using vernier calipers might be limited to a small visible subpart of the infiltrated area. Especially, if the cancer cell density of the originated invasive cancer cells is too small to be detected, the injected initial tumour mass might be the only part of the tumour, that can be measured with vernier calipers.
The proposed model is easy to extend. For instance, cells produce ECM reducing metallo-matrix proteins or they change the metabolism to an oxygen independent but acidic lactate producing modus. Both weaken the mechanical properties of the ECM. The first reduces the amount of solid material, the second changes the material properties of the solid phase due to an acidic environment (Achilli and Mantovani (2010)). Parameters can be modified based on environmental concentrations, and mass exchange terms can easily be added to take into account the degradation of solid material. Besides the cells' impact on the environment, the environmental feedback on the cells can be considered. The model calculates the interstitial fluid pressure as well as the oxygen concentration to any discrete time step. The increasing interstitial fluid pressure does not have only an effect on the drug efficiency (Heldin et al. (2004)) but is also connected to the pressure induced crosslinking of ECM molecules. This crosslinking activates the mechano signal transduction, which activates proto-oncogene tyrosine-protein kinase SRC (Levental et al. (2009)), a protein that is also triggered by limited oxygen concentration (Hanna et al. (2013)). This will be modelled in subsequent papers as concentration of active SRCa depending on ECM displacement $[SRCa] \propto \mathbf{u}^s$. SRC is directly responsible for the loose of cell-cell contacts and migration (Avizienyte and Frame (2005)), which we can in turn consider as viscosity change. SRC activates extracellular signal-regulated kinase (ERK), which is, with its interacting partners, a central player in cancer biology and a target for pharmaceuticals. Moreover, our model provides at any time the relation between interstitial fluid, tumour cytoplasm and host cell cytoplasm, which can be used to relate quantitatively the intracellular pathways to each other, *e.g.* based on the input-output behaviour of molecular network models. The per cell production rate of any molecule can be directly translated to the actual concentration in the limited interstitial volume.

6. CONCLUSION

The thermodynamically constrained averaging theory has been used to model cancer growth in three dimensional collagen gels or tissues. The benefit of our modelling approach is, that the ECM and the host cells can be actuated separately by the cancer cells, while most other continuous modelling approaches treat the environment as a mixture with averaged material properties. This allows us to use the advantages of continuous and bio mechanical modelling while reaching additional advantages of agent-based

modelling. While the agent-based models define clearly the reaction volume of each cell, we define clearly the reaction volumes of the cytoplasm within a representative volume element. This can be justified if neither single cell information is available nor cellular memory must be tracked. While in agent-based systems the number of cell types are nearly unlimited, our described cell liquids can be subdivided in several miscible and cell type specific liquids. Our approach shifts the focus on inter cell communication to a more holistic view with cell-ECM interplay. This improves the modelling for cancer growth in comparison to agent-based models with its accumulation of mechanical deformable beads and in comparison to other continuous models without clear definition of reaction spaces, molecular networks relate to. The reduction of cell-cell contacts and the reduction of the intracellular stiffness reduce the overall viscosity of the tumour cell population. The TCAT parameter viscosity is a central player for the tumour growth shape and the overall tumour volume. A low viscosity reduces the displacement of the ECM and the tumour cells infiltrate a much larger volume. Due to a changed oxygen profile in the low viscous tumour, the cancer cell density within the tumour remains small. The parameter viscosity can be linked with several biologically meaningful sub-systems or molecules and the proposed model has the potential to extend network orientated models, formulated in the field of Systems Biology.

ACKNOWLEDGEMENTS

This work has been financed by the European Union. We acknowledge the Horizon 2020 MSCA grant agreement, No 642295, www.melplex.eu. Moreover, we thank the Fonds National de la Recherche, Luxembourg (INTER/BMBF/13/03).

REFERENCES

Achilli, M. and Mantovani, D. (2010). Tailoring mechanical properties of collagen-based scaffolds for vascular tissue engineering: the effects of ph, temperature and ionic strength on gelation. *Polymers*, 2(4), 664–680.

Avizienyte, E. and Frame, M.C. (2005). Src and FAK signalling controls adhesion fate and the epithelial-to-mesenchymal transition. *Current opinion in cell biology*, 17(5), 542–547.

Butcher, D.T., Alliston, T., and Weaver, V.M. (2009). A tense situation: forcing tumour progression. *Nature Reviews Cancer*, 9(2), 108–122.

Frieboes, H.B., Chaplain, M.A., Thompson, A.M., Bearer, E.L., Lowengrub, J.S., and Cristini, V. (2011). Physical oncology: a bench-to-bedside quantitative and predictive approach. *Cancer research*, 71(2), 298–302.

Gray, W.G. and Miller, C.T. (2014). *Introduction to the thermodynamically constrained averaging theory for porous medium systems*. Springer.

Greaves, M. and Maley, C.C. (2012). Clonal evolution in cancer. *Nature*, 481(7381), 306–313.

Guck, J., Schinkinger, S., Lincoln, B., Wottawah, F., Ebert, S., Romeyke, M., Lenz, D., Erickson, H.M., Ananthakrishnan, R., Mitchell, D., et al. (2005). Optical deformability as an inherent cell marker for testing malignant transformation and metastatic competence. *Biophysical journal*, 88(5), 3689–3698.

Hanna, S.C., Krishnan, B., Bailey, S.T., Moschos, S.J., Kuan, P.F., Shimamura, T., Osborne, L.D., Siegel, M.B., Duncan, L.M., O'Brien, E.T., et al. (2013). HIF1α and HIF2α independently activate SRC to promote melanoma metastases. *The Journal of clinical investigation*, 123(5), 2078–2093.

Hatzikirou, H., Chauviere, A., Bauer, A.L., Leier, A., Lewis, M.T., Macklin, P., Marquez-Lago, T.T., Bearer, E.L., and Cristini, V. (2012). Integrative physical oncology. *Wiley Interdisciplinary Reviews: Systems Biology and Medicine*, 4(1), 1–14.

Heldin, C.H., Rubin, K., Pietras, K., and Östman, A. (2004). High interstitial fluid pressure- an obstacle in cancer therapy. *Nature Reviews Cancer*, 4(10), 806–813.

Hoek, K.S., Eichhoff, O.M., Schlegel, N.C., Döbbeling, U., Kobert, N., Schaerer, L., Hemmi, S., and Dummer, R. (2008). In vivo switching of human melanoma cells between proliferative and invasive states. *Cancer research*, 68(3), 650–656.

Humphrey, J.D., Dufresne, E.R., and Schwartz, M.A. (2014). Mechanotransduction and extracellular matrix homeostasis. *Nature Reviews Molecular Cell Biology*, 15(12), 802–812.

Levental, K.R., Yu, H., Kass, L., Lakins, J.N., Egeblad, M., Erler, J.T., Fong, S.F., Csiszar, K., Giaccia, A., Weninger, W., et al. (2009). Matrix crosslinking forces tumor progression by enhancing integrin signaling. *Cell*, 139(5), 891–906.

Macklin, P., Mumenthaler, S., and Lowengrub, J. (2013). Modeling multiscale necrotic and calcified tissue biomechanics in cancer patients: application to ductal carcinoma in situ (DCIS). In *Multiscale computer modeling in biomechanics and biomedical engineering*, 349–380. Springer.

Sciumè, G., Boso, D., Gray, W.G., Cobelli, C., and Schrefler, B. (2014a). A two-phase model of plantar tissue: a step toward prediction of diabetic foot ulceration. *International journal for numerical methods in biomedical engineering*, 30(11), 1153–1169.

Sciumè, G., Gray, W.G., Ferrari, M., Decuzzi, P., and Schrefler, B. (2013). On computational modeling in tumor growth. *Archives of Computational Methods in Engineering*, 20(4), 327–352.

Sciumè, G., Santagiuliana, R., Ferrari, M., Decuzzi, P., and Schrefler, B. (2014b). A tumor growth model with deformable ECM. *Physical biology*, 11(6), 065004.

Stylianopoulos, T., Martin, J.D., Chauhan, V.P., Jain, S.R., Diop-Frimpong, B., Bardeesy, N., Smith, B.L., Ferrone, C.R., Hornicek, F.J., Boucher, Y., et al. (2012). Causes, consequences, and remedies for growth-induced solid stress in murine and human tumors. *Proceedings of the National Academy of Sciences*, 109(38), 15101–15108.

Weder, G., Hendriks-Balk, M.C., Smajda, R., Rimoldi, D., Liley, M., Heinzelmann, H., Meister, A., and Mariotti, A. (2014). Increased plasticity of the stiffness of melanoma cells correlates with their acquisition of metastatic properties. *Nanomedicine: Nanotechnology, Biology and Medicine*, 10(1), 141–148.